VOL. 77, NO. 32 JOURNAL OF GEOPHYSICAL RESEARCH NOVEMBER 10, 1972

Measurement of Single-Crystal Elastic Constants of Bronzite as a Function of Pressure and Temperature

A. L. FRISILLO[1] AND G. R. BARSCH[2]

Materials Research Laboratory, The Pennsylvania State University
University Park, Pennsylvania 16802

The nine single-crystal elastic constants of orthopyroxene, $Mg_{0.8}Fe_{0.2}SiO_3$, have been measured as a function of temperature from 25° to 350°C and at 25°C as a function of pressure to 10 kb by means of the ultrasonic pulse superposition technique. It was found that the shear constants exhibited a distinctly nonlinear pressure dependence in addition to the usual linear terms. Owing to the difficulty in obtaining precise data for the longitudinal modes above approximately 4.5 kb, where curvature might be observed, only a linear pressure dependence was found for the on-diagonal longitudinal constants. Because the second pressure derivatives of the on-diagonal longitudinal constants (c_{11}, c_{22}, and c_{33}) enter the expressions required for the evaluation of the second pressure derivatives of the off-diagonal constants (c_{12}, c_{23}, and c_{13}), the second derivatives of the off-diagonal constants are probably considerably in error. The second pressure derivatives of the on-diagonal shear constants and of the unprocessed data for the cross-coupling moduli, however, have been precisely and consistently measured and represent the first observations of curvature for noncubic oxide materials. The dimensionless quantities $K(\partial c_{\mu\nu}/\partial P^2)$ (where K denotes the bulk modulus, $c_{\mu\nu}$ denotes the elastic constants, and P denotes the pressure) for the on-diagonal shear moduli are about ten times larger than the corresponding quantities for the eight alkali halides for which these quantities are known. The isotropic bulk and shear moduli and their pressure and temperature derivatives calculated from the single-crystal data by means of the Voigt-Reuss-Hill (VRH) approximation are $K^s = 1.035$ Mb, $G = 0.749$ Mb, $(\partial K^s/\partial P)_T = 9.59$, $(\partial G/\partial P)_T = 2.38$, $(\partial K^s/\partial T)_p = -0.268$ kb°C^{-1}, and $(\partial G/\partial T)_p = -0.119$ kb°C^{-1}. Owing to the large values of the pressure derivatives of the longitudinal elastic constants c_{11}, c_{22}, and especially c_{33}, the pressure derivative of the bulk modulus of orthopyroxene is approximately twice as large as that for most other materials normally considered to be of importance in the earth's mantle. The ultrasonic equation of state calculated from the first-order Birch equation agrees well with static-compression data and, below about 150 kb, with shock-wave data. The elastic Grueneisen parameter calculated from the VRH approximation is found to be 30% larger than the thermal Grueneisen parameter.

The single-crystal elastic constants of many geophysically relevant materials have been ultrasonically measured by several authors as a function of temperature and pressure (see, for example, the compilations by *Hearmon* [1969] and *Bechmann* [1969] and, in addition, those by *Graham and Barsch* [1969] and *Kumazawa and Anderson* [1969]). Available single-crystal elastic data on pyroxenes, however, have been limited by the paucity of suitable specimens of sufficient size and quality on which to perform ultrasonic measurements. Single-crystal data have been reported for six clinopyroxenes [*Alexandrov and Ryzhova*, 1961; *Alexandrov et al.*, 1963] and two orthopyroxenes of the bronzite variety [*Ryzhova et al.*, 1966; *Kumazawa*, 1969]. In none of these studies, however, were the effects of elevated temperature and pressure included. For orthopyroxene the temperature and pressure dependence of compressional- and shear-wave velocities has been measured [*Birch*, 1960; *Simmons*, 1964; *Hughes and Nishitake*, 1963]. These measurements, however, have been made on natural rock specimens in which the problems of porosity, cracks, heterogeneity, and large grain size reduce the precision of the measurements, particularly those of the temperature and pressure derivatives. In addition, compressional- and shear-wave velocity

[1] Also affiliated with Department of Geosciences. Now at NASA Manned Spacecraft Center, Houston, Texas 77058.

[2] Also affiliated with Department of Physics.

TABLE 1. Quantitative Analysis of Bronzite Specimens by Atomic Absorption (All values in wt %.)

Element	Sample 1	Sample 2	Sample 3	Sample 4	Maximum Difference
MgO	30.10	28.80	30.30	30.80	2.0
SiO_2	54.80	53.80	54.00	54.00	1.0
Fe_2O_3*	13.60	13.90	14.90	14.40	1.3
Al_2O_3	0.60	0.68	1.00	0.79	0.4
CaO	0.18	0.29	0.50	0.50	0.04
MnO	0.24	0.28	0.25	0.24	0.04
Na_2O	0.00	0.00	0.43	0.09	0.43
BaO	0.00	0.00	0.04	0.04	0.04
NiO	0.06	0.00	0.00	0.00	0.06
Total	99.58	97.75	101.42	100.86	

Detected spectrographically in trace amounts for all samples: Cr, V, Zn, Zr, Co, Cu, Ti.
*All iron expressed as ferrous iron.

data as well as temperature and pressure dependence were obtained from different specimens with varying compositions by several investigators. Therefore, for a more complete understanding of materials thought to be of importance in the earth's mantle, it is necessary to obtain elasticity data for members of the pyroxene family as a function of temperature and pressure. The purpose of this paper is to present precise data for the single-crystal elastic constants of natural orthopyroxene and their temperature and pressure derivatives.

Experimental Procedure

Four natural single-crystal orthopyroxene samples from India (purchased from the Commercial Mineral Company, New York) were used in this investigation. A quantitative analysis using atomic absorption was performed by R. E. Raver of the Pennsylvania State University Mineral Constitution Laboratory (Table 1). The mean molecular formula as determined from these data is approximately $Mg_{0.8}Fe_{0.2}SiO_3$. The specimens are therefore of the bronzite variety.

Orthopyroxene belongs to the orthorhombic space group *Pbca* [*Wyckoff*, 1968]. Therefore nine second-order elastic constants are necessary to describe the elastic behavior of the crystal. In the Voigt notation they are c_{11}, c_{22}, c_{33}, c_{44}, c_{55}, c_{66}, c_{12}, c_{13}, and c_{23}. All the on-diagonal moduli $c_{\mu\mu}$ (no summation convention) can be determined from ultrasonic velocity measurements in pure-mode directions parallel to the crystallographic a, b, and c axes, which also provide cross checks on c_{44}, c_{55}, and c_{66}. The three cross-coupling moduli (c_{12}, c_{13}, and c_{23}) can be determined from three different propagation directions perpendicular to one of the orthogonal crystallographic axes and oblique to the remaining two. Therefore three different orientations are necessary to determine the cross-coupling moduli in addition to the pure-mode orientations. The equations used for the calculation of the elastic constants and their first and second pressure derivatives for these orientations can be determined from the Christoffel equations and have been given by *Fisher and McSkimin* [1958], *Graham* [1969], and *Barsch and Frisillo* [1973]. Because no single specimen was large enough to determine all nine of the elastic constants and because the specimens have approximately the same chemical composition, it was decided to use all four specimens.

Figure 1 illustrates the orientation of the four samples. Specimen 1 was used for determining the on-diagonal moduli, and specimens 2, 3, and 4 were used for determining the cross-coupling moduli. In addition, propagation directions parallel to the x axis for specimens 2, 3, and 4 (Figure 1) were also used to measure the respective on-diagonal moduli, which could then be compared with data from specimen 1. In this way the results from the four different

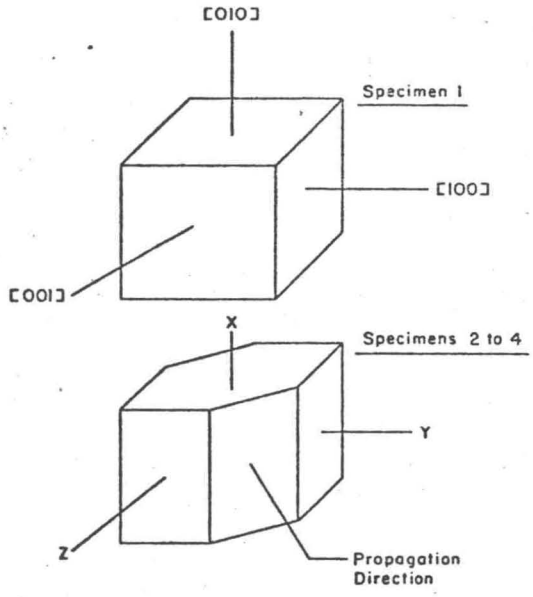

Specimen	X	Y	Z
2	[001]	[010]	[100]
3	[100]	[010]	[001]
4	[010]	[100]	[001]

Fig. 1. Orientation of specimens used for the elastic-constant measurements.

samples could be examined for consistency. Sample 2, which would have been used to determine the on-diagonal moduli corresponding to the [001] propagation direction, cleaved while it was being ground. As a result, further attempts at grinding the (001) face were not made. Specimens 3 and 4, however, were successfully prepared, and checks could be made on the elastic constants obtained from propagation directions parallel to [100] and [010].

All sample faces were oriented by using the Laue back-reflection technique and are accurate to better than 1°. The faces of the samples were ground flat by using #320 silicon carbide powder and were polished with 1-μ diamond paste. The sample faces were found to be parallel to within 0.0001 cm/cm and flat to within 0.0001 cm. Sample thickness was measured by using a Starrett 221 micrometer with a stated accuracy of $\pm$0.00003 cm. The densities of the specimens were determined by using the usual liquid immersion method (Table 2). A mean density of 3.354 $\pm$ 0.002 g/cm^3 was adopted for all calculations.

The adiabatic elastic constants and their temperature and pressure dependence were determined by measuring the transit times of 20-MHz ultrasonic waves between parallel faces by using the pulse superposition technique of *McSkimin* [1961]. Two different ultrasonic pulse superposition units, which have been designated MRL PSP AFC and Arenberg PSP AFC, were used in the present study. Unless it is otherwise specified, the MRL unit has been used to obtain the acoustic data presented in this study. A complete description of these units, including the automatic peak finder, which electronically detects the correct echo maximum, has been given in detail by other authors [*Gieske*, 1968; *Miller*, 1969]. The pressure apparatus has been described previously by *Bogardus* [1964].

For determining the zero pressure elastic constants and during the pressure tests, the temperature of the specimens was maintained at 25.0 $\pm$ 1.0°C by circulating water through a copper tubing jacket wrapped around the outside of the pressure vessel with a Lauda constant temperature circulator (model NBS-HT). The temperature and the temperature gradient of the specimens were monitored by two chromel-alumel thermocouples placed in proximity to two different faces of the specimen. The thermal emf's were measured before and after each measurement on a Leeds and Northrup K-3 potentiometer by using an ice bath reference, and a negligible temperature gradient was indicated within the specimens.

Pressure in the vessel was provided by compressing argon gas with a Harwood two-stage gas compressor system. The pressure in the test vessel was measured by a manganin cell in conjunction with a Carey-Foster bridge (model C, Harwood Engineering Company) calibrated prior to each pressure run.

The temperature dependence of the elastic constants was determined by using an internal furnace made of a cylindrically wound coil of

TABLE 2. Densitites of Bronzite Specimens at 25°C

Specimen	Density, g/cm^3
1	3.354 ± 0.001
2	3.355 ± 0.001
3	3.355 ± 0.001
4	3.351 ± 0.001
Average	3.354 ± 0.002

Kanthal wire that fits within the 2-inch diameter of the bore of the pressure vessel. By using the thermocouple arrangement described for the pressure tests, a maximum variation of ±1.5°C was maintained during all temperature measurements. To minimize the effects of oxidation of the bore and the sample-holding device, the system was purged with argon gas prior to each temperature run. Natural quartz ac- and cross-cut transducers having diameters of 0.250 inch and resonance frequencies of 20 MHz ± 1% (purchased from the Valpey Corporation, Holliston, Massachusetts) were used to generate and receive the transverse and longitudinal ultrasonic wave pulses, respectively. Two types of bonding materials were used to cement the transducers to the sample faces. At room temperature, for measuring the elastic constants and their pressure dependence, non-aq stopcock grease (Fisher Scientific Company) was used. For high-temperature measurements Extemp 9901 (Lubrication Engineering Company) was found to be satisfactory to approximately 350°C, at which point it became dry and was no longer functional.

EXPERIMENTAL RESULTS

Elastic constants at 25°C and 1 atm. By using the orientations shown in Figure 1 and the equations of *Fisher and McSkimin* [1958], the adiabatic elastic constants $c_{\mu\nu}{}^S$ were determined (Table 3). The corresponding sample numbers, propagation directions **N**, and polarization directions **U** used to obtain the $c_{\mu\nu}{}^S$ are also included in this table. When it is considered that four different natural specimens were used, the consistency of the data is quite remarkable.

Because calculation of the cross-coupling moduli depends on the direction cosines of the propagation directions, it is necessary to determine these quantities accurately. They were determined by the method proposed by *Fisher and McSkimin* [1958]. Because each cross-coupling modulus may be determined by either a 'quasi-shear' or a 'quasi-longitudinal' elastic-wave velocity, the propagation angles and the associated elastic constants can be calculated simultaneously. The calculated angles and the pure transverse mode cross check afforded by the pure transverse mode relations are listed in Tables 4 and 5. Despite small compositional variations, the method of Fisher and McSkimin leads to a maximum difference of only 0.6% in the calculated and measured values of ρV^2 (Table 4). This check justifies the application of this method, even though four different specimens were used.

TABLE 3. Velocities of Pure Modes and Calculated Values of the Adiabatic On-Diagonal Elastic Constants at 25°C

Elastic Constant	Sample	$\hat{N}$	$\hat{U}$	Thickness d, mm	Velocity, km/sec	$c_{\mu\mu}{}^S$, Mb	Average $c_{\mu\mu}{}^S$, Mb
c_{11}	3	[100]	[100]	6.696	8.255	2.286	2.286 ± 0.001
	1	[100]	[100]	6.794	8.253	2.285	
c_{22}	4	[010]	[010]	7.176	6.915	1.604	1.605 ± 0.001
	1	[010]	[010]	7.664	6.920	1.606	
c_{33}	1	[001]	[001]	6.783	7.920	2.104	2.104 ± 0.001*
c_{44}	1	[010]	[001]	7.664	4.934	0.8167	
	4	[010]	[001]	7.176	4.940	0.8184	0.8175 ± 0.0009
	1	[001]	[010]	7.683	4.936	0.8174	
c_{55}	1	[100]	[001]	6.794	4.745	0.7553	
	3	[100]	[001]	6.696	4.744	0.7551	0.7548 ± 0.0007
	1	[001]	[100]	7.683	4.741	0.7541	
c_{66}	1	[100]	[010]	6.794	4.814	0.7772	
	3	[100]	[010]	6.696	4.809	0.7759	0.7766 ± 0.0005
	1	[010]	[100]	7.664	4.810	0.7763	
	4	[010]	[100]	7.196	4.813	0.7768	

*Error assumed to be equal to that of c_{11} and c_{22}.

TABLE 4. Calculated Propagation Directions for Cross-Coupling Constants and Associated Pure-Mode Checks

Associated Elastic Constant	Sample	$\vec{N}$	Direction Cosine	Angle	Pure-Mode Relation	Calculated ρV^2, Mb	Measured ρV^2, Mb
c_{13}	4	$[l0n]$	$l = 0.8332$ $n = 0.5529$	33°34' 56°26'	$l^2c_{66} + n^2c_{44} = \rho_0 V_{S2}^2$	0.7910	0.7960
c_{12}	2	$[lm0]$	$l = 0.7437$ $m = 0.6685$	41°57' 48°03'	$l^2c_{55} + m^2c_{44} = \rho_0 V_{S3}^2$	0.7828	0.7874
c_{23}	3	$[0mn]$	$m = 0.7590$ $n = 0.6510$	40°37' 49°23'	$m^2c_{66} + n^2c_{55} = \rho_0 V_{S1}^2$	0.7673	0.7664

The known experimental errors occurring for the elastic-constant measurements are 0.02% for specimen thickness, 0.003% for specimen orientation, and 0.06% for specimen density. Because many of the moduli were measured on two sets of ultrasonic units that gave results identical to those in Table 3, systematic errors resulting from the ultrasonic equipment are considered negligible. Adding the known experimental errors gives a total probable error of 0.083%. Although this estimate of the known experimental error is a generous one, it does not completely account for the experimentally observed deviations in the values of the elastic constants. This fact, however, is not surprising, since four different specimens of slightly different compositions were used in this study. Because an appropriate compositional correction is not known, possible errors occurring in the measurements owing to compositional variations cannot be accounted for. In addition, because slight inhomogeneities are known to occur for most natural specimens, a second possible unknown correction term must be ignored. Consequently, a comprehensive estimate of the probable error in the experimental determination of the elastic constants is not possible. As a result, the scatter in the values obtained from the various modes and the cross checks for the on-diagonal moduli are taken to be indicative of the probable error in their measurements.

Because the equations used for calculating the cross-coupling moduli depend on other on-diagonal moduli, on the direction cosines, and on the measured values of ρV^2, it is apparent that their associated probable errors are considerably larger than those for the on-diagonal moduli. A reasonable estimate of the probable errors for the cross-coupling moduli may be determined from the Gaussian error propagation law. In this manner the probable errors given in Table 5 were obtained from the errors

TABLE 5. Velocities of Quasi-Modes and Calculated Values of the Adiabatic Cross-Coupling Elastic Constants at 25°C

Elastic Constant	Sample	$\vec{N}$	Thickness d, mm	Velocity, km/sec	$c_{\mu\nu}^S$, Mb
c_{23}	3	$[0mn]$	8.641	$V_{QS} = 4.515$ $V_{Qp} = 7.624$	0.460 ± 0.002
c_{13}	4	$[l0n]$	5.054	$V_{QS} = 4.914$ $V_{Qp} = 8.055$	0.548 ± 0.002
c_{13}	2	$[lm0]$	6.588	$V_{QS} = 4.245$ $V_{Qp} = 8.014$	0.710 ± 0.002

of the on-diagonal moduli, ρV^2, and the direction cosines.

Pressure dependence of effective second-order elastic constants. The basic data necessary to determine the isothermal pressure derivatives of the effective second-order adiabatic elastic constants are the transit time of the ultrasonic wave at elevated pressure t_r and the specimen thickness at zero pressure d_0. From these data the natural wave velocity W [*Thurston and Brugger*, 1964] can be calculated at each experimental pressure by using $W = 2d_0/t_r$. The pressure dependence of the quantity $\rho_0 W^2$ can be expressed by the first N expansion terms of the Taylor series:

$$\rho_0 W^2 = \rho_0 \sum_{n=0}^{N} A_n{}^N (P^n/n!) \qquad (1a)$$

$$\rho_0 W^2 = \rho_0 W_0{}^2 + (\rho_0 W^2)' P + (\rho_0 W^2)'' P^2/2 + \cdots \qquad (1b)$$

The first term on the right-hand side of (1*b*) represents the zero pressure value of the respective on-diagonal elastic constant, or the quantities $\rho_0 V_{QS}{}^2$ or $\rho_0 V_{QP}{}^2$ used in computing the off-diagonal moduli. The remaining two quantities, $(\rho_0 W^2)'$ and $(\rho_0 W^2)''/2$, are, according to the equations of *Graham* [1969] and *Barsch and Frisillo* [1972], related to the first and second pressure derivatives of the elastic constants, respectively.

In this study all data were fitted to first-, second-, and third-order polynomials, and the resulting coefficients and standard deviations were examined for best fit. On the basis of the criteria discussed in the appendix, the data for the longitudinal modes are found to fit the first-order polynomial best in all cases. The data for the shear and quasi-shear modes, however, required a second-order fit, and thus a statistically significant nonlinearity was indicated. As is shown in the appendix, a fit to a third-order

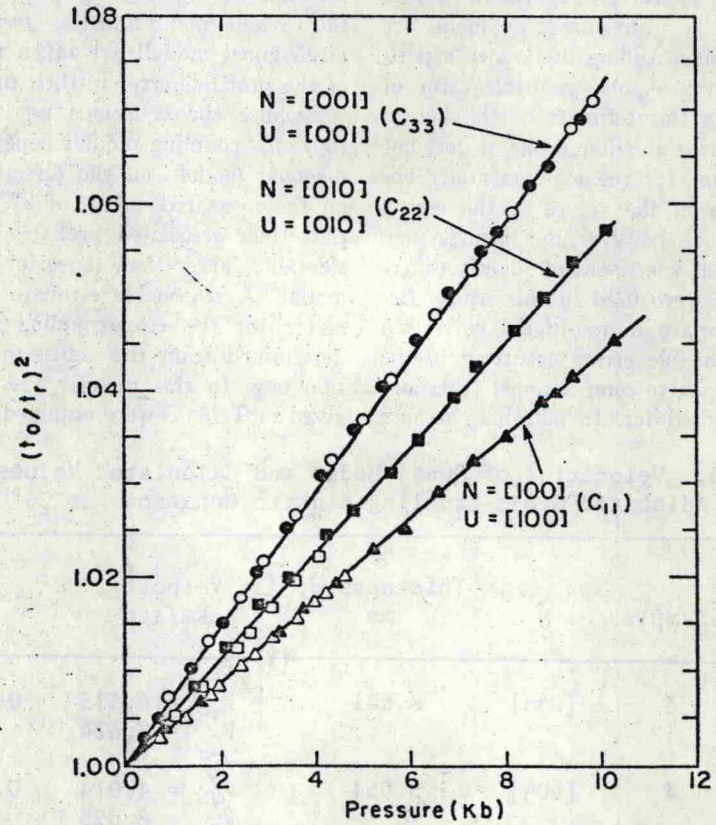

Fig. 2. Experimental data of $(t_0/t_r)^2$ as a function of pressure for the on-diagonal moduli c_{11}, c_{22}, and c_{33}. Solid and open circles, solid triangles, and open squares indicate specimen 1; open triangles, specimen 3; solid squares, specimen 4.

polynomial could not be justified for any of the shear or quasi-shear modes, with the exception of three modes belonging to the moduli c_{44} and c_{55}. These three modes represent borderline cases and were for the sake of uniformity also fitted to second-order polynomials.

In all, 23 pressure tests were performed on the four specimens used in this study. In this way many cross checks of the pressure dependence of the elastic constants resulting from different propagation directions in the specimens could be examined for consistency. As typical examples of unprocessed pressure data, the normalized quantity $(t_0/t_r)^2 = (W/W_0)^2$, where t_0 denotes the transit time at zero pressure, is plotted versus pressures for the modes corresponding to the on-diagonal longitudinal moduli (Figure 2) and for those corresponding to the shear modulus c_{55} and the cross-coupling modulus c_{13} (Figure 3). To illustrate the nonlinearity for the shear modes, the initial slope for N = [001] and U = [100] (c_{55}) (Figure 3) has been linearly extrapolated to higher pressures. It is also apparent (Figure 3) that the quasi-shear mode corresponding to c_{13} also shows a distinctly nonlinear behavior. All solid lines in this figure represent the quadratic least-squares fit according to

$$(W/W_0)^2 = (t_0/t_r)^2 = 1 + (W^2/W_0^2)'P + (W^2/W_0^2)''P^2/2 \quad (2)$$

For calculating the first pressure derivatives of the elastic constants from the measured values of $(\rho_0 W^2)'$, the isothermal single-crystal bulk modulus K_0^T and the isothermal compliance coefficients $S_{\mu\nu}^T$ are required. The adiabatic single-crystal bulk modulus can be determined from the general expression

$$K_0^S = (S_{iiii}^S)^{-1} \quad (3)$$

and converted to its isothermal counterpart by *Overton*'s [1962] equation 2. This equation gives $K_0^S = 1.021$ Mb and $K_0^T = 0.998$ Mb.

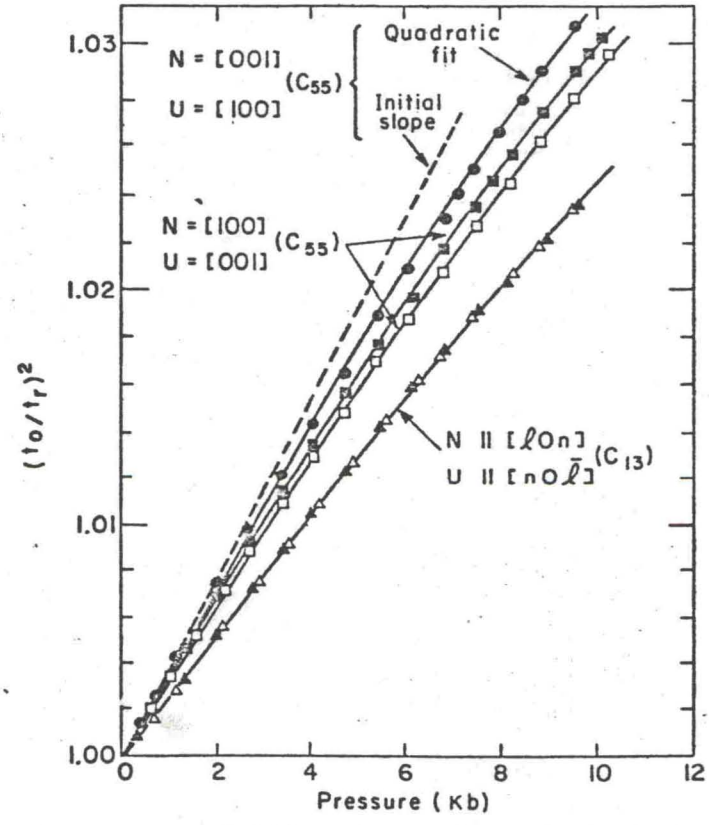

Fig. 3. Experimental data of $(t_0/t_r)^2$ as a function of pressure for the elastic moduli c_{55} and c_{13}. Solid squares and solid circles indicate specimen 1; open squares, specimen 3; solid and open triangles, specimen 4.

TABLE 6. Adiabatic and Isothermal Elastic Compliance Coefficients at 25°C (All values in Mb^{-1}.)

Coefficient	Adiabatic	Isothermal
s_{11}	0.5253	0.5259
s_{22}	0.7453	0.7474
s_{33}	0.5231	0.5259
s_{44}	1.223	1.223
s_{55}	1.325	1.325
s_{66}	1.288	1.288
s_{12}	-0.2053	-0.2029
s_{13}	-0.0914	-0.0886
s_{23}	-0.1095	-0.1070

The adiabatic compliance coefficients can be determined by inversion of the adiabatic elastic-constant matrix, and the isothermal compliance coefficients can be calculated from *Thurston* [1967]:

$$S_{ijkl}{}^{T} = S_{ijkl}{}^{S} + (T\alpha_{ij}\alpha_{kl}/\rho_0 C_P) \qquad (4)$$

where α_{ij} are the linear thermal-expansion coefficients, T is the temperature, and C_p is the specific heat at constant pressure. The thermal-expansion coefficients of bronzite used were determined by *Frisillo and Buljan* [1972], and the specific heat was calculated from the present elastic data [*Anderson*, 1965]. The value obtained for $C_p = 94.66$ mole^{-1} °K^{-1}. The adiabatic elastic compliances are tabulated in Table 6 together with the isothermal values calculated from the preceding data.

First pressure derivatives of effective second-order elastic constants. The isothermal first pressure derivatives of the adiabatic effective elastic constants were calculated by using the equations given by *Graham* [1969] and *Barsch and Frisillo* [1973] (Table 7). The internal cross checks resulting from orthorhombic symmetry coupled with checks from the four different specimens show excellent agreement in the computed values.

Because an intercrystal check on the pressure derivatives of c_{33} was not possible, the reliability of the measured values was examined by making two independent pressure runs. Although the cross-coupling moduli may also be determined by propagation of quasi-longitudinal modes, their echoes became very small and nondistinct at pressures of about 4.5 kb and were not detected by the automatic peak finder. Because this phenomenon was observed for all longitudinal pressure runs, all longitudinal data above approximately 4.5 kb were taken manually (i.e., without the automatic peak finder). Because a small but significant amount of curvature was observed for all shear moduli and because the manually taken data were not precise enough to describe this curvature, consistency for the pressure derivatives of the cross-coupling coefficients was again determined by repeating the quasi-shear pressure runs. A single quasi-longitudinal run was performed for propagation direction $\mathbf{N} = [0mn]$ and polarization $\mathbf{U} = [0mn]$ and was then used as a consistency check for $(\partial c_{23}/\partial P)_T = c_{23}'$ and as an independent check on the accuracy of c_{33}'. An independent check on c_{33}' results from considering the expressions given by *Fisher and McSkimin* [1958] to calculate the direction cosines for propagation direction $\mathbf{N} = [0mn]$:

$$m^2 = \frac{\rho V_{QS}{}^2 + \rho V_{QP}{}^2 - (c_{33}{}^S + c_{44}{}^S)}{c_{22}{}^S - c_{33}{}^S} \qquad (5)$$

where $m^2 + n^2 = 1$. By differentiating (5) with respect to pressure and solving for c_{33}', the following expression is obtained:

$$c_{33}' = \{[(\rho V_{QP}{}^2)' + (\rho V^2)_{QS}' - c_{44}']n - (\rho V_{QP}{}^2 + \rho V_{QS}{}^2 - c_{44})2n' - (2m'c_{22} + mc_{22}')nm + 2m^2n'c_{22}\}/n^3 \qquad (6)$$

Here m' and n' denote the first pressure derivatives of the direction cosines, which can be cal-

TABLE 7. Isothermal First Pressure Derivatives of the Effective Elastic Constants at 25°C

$c_{\mu\nu}$	Specimen	$\vec{N}$	$\vec{U}$	$[\partial(\rho_0 W^2)/\partial P]_0$	$(\partial c_{\mu\nu}{}^S/\partial P)_0$	Weighted Average
c_{11}	3	[100]	[100]	9.86	11.08 ± 0.06	11.04 ± 0.06
	1	[100]	[100]	9.72	10.94 ± 0.09	
c_{22}	1	[010]	[010]	9.07	9.27 ± 0.07	9.19 ± 0.08
	4	[010]	[010]	8.90	9.11 ± 0.07	
c_{33}	1	[001]	[001]	15.69	16.40 ± 0.06	16.42 ± 0.04
	1	[001]	[001]	15.72	16.44 ± 0.06	
c_{44}	1	[010]	[001]	2.25	2.35 ± 0.01	2.38 ± 0.03
	4	[010]	[001]	2.36	2.46 ± 0.01	
	1	[001]	[010]	2.08	2.36 ± 0.01	
	1*	[001]	[010]	2.12	2.40 ± 0.02	
c_{55}	1	[100]	[001]	2.58	2.98 ± 0.01	2.92 ± 0.04
	3	[100]	[001]	2.45	2.85 ± 0.01	
	1	[001]	[100]	2.71	2.97 ± 0.02	
c_{66}	1	[100]	[010]	2.36	2.77 ± 0.01	2.75 ± 0.01
	3*	[100]	[010]	2.35	2.77 ± 0.01	
	1	[010]	[100]	2.61	2.71 ± 0.02	
	4	[010]	[100]	2.61	2.71 ± 0.02	
c_{12}	2	$[lm0]$	$[m\bar{l}0]$	1.66	6.97 ± 0.14	6.97 ± 0.10
	2*			1.66	6.97 ± 0.14	
c_{13}	4*	$[l0n]$	$[n0\bar{l}]$	2.21	9.11 ± 0.14	9.09 ± 0.10
	4*			2.19	9.07 ± 0.14	
c_{23}	3	$[0mn]$	$[0n\bar{m}]$	1.64	8.69 ± 0.10	8.73 ± 0.10
	3*			1.57	8.83 ± 0.15	

*Run made with Arenberg PSP AFC ultrasonic equipment. All other data were taken with MRL PSP AFC equipment.

culated from the isothermal elastic compliances [*Graham*, 1969; *Barsch and Frisillo*, 1973]. The computed cross checks $c_{22}' = 8.72$ and $c_{33}' = 16.53$ are in excellent agreement with their corresponding values in Table 7. The agreement of the check on c_{33}' illustrates the self-consistency of the data, since knowledge of c_{44} and c_{22} and of their first pressure derivatives is required for the calculation.

To test the possibility of inherent systematic error in the MRL PSP AFC ultrasonic equipment used to obtain most of these data, several pressure runs were made with a different ultrasonic unit (Arenberg PSP AFS). The agreement of the data obtained by using the two ultrasonic units demonstrates that systematic errors from the electronic system are very small.

The errors shown in Table 7 for $(\partial c\mu\nu'/\partial P)_0$ are based on the standard deviations of the least-squares curve fit of $(\rho W^2)_0'$. Because the major source of error in $(\rho V^2)_0'$ arises from $(\rho W^2)_0'$, the standard deviation of the curve fitted to the raw data can be considered as a reasonable estimate of the probable error for each run. The error given for the cross-coupling moduli was determined from the errors of $(\rho_0 W^2)_0'$, of the pressure coefficient of the on-diagonal moduli, and of the direction cosines by means of the Gaussian error propagation law. In several cases the differences between the value of $(\partial c_{\mu\nu}{}^S/\partial P)_0$ obtained from different modes are larger than the standard errors of the individual runs. Therefore the 'weighted average' values $\langle V \rangle$ were determined by

$$V = \sum_{i=1}^{n} W_i V_i \Big/ \sum_{i=1}^{n} W_i \qquad (7)$$

where $W_i = 1/(\text{s.d.})^2$ for the individual runs and V_i are the corresponding values of $(\partial c_{\mu\nu}{}^S/\partial P)_0$ to be averaged. The errors for the weighted average values were estimated according to

$$\Delta = \left[\sum_{i=1}^{n} W_i[(V_i - \langle V \rangle)^2 + \sigma_i^2]/n \sum_{i=1}^{n} W_i \right]^{1/2} \quad (8)$$

where σ_i is the standard error of each value V_i and n is the number of modes to be averaged. (This formula has been suggested to the authors by H. H. Demarest, Jr.) This formula is a useful extension of the Gaussian error propagation law to which it reduces in the case of perfect consistency ($V_i = \langle V \rangle$ for all i). Its validity is restricted to the case of good consistency ($(V_i - \langle V \rangle)^2 < \sigma_i^2$). For 'inconsistent' data ($(V_i - \langle V \rangle)^2 > \sigma_i^2$) the factor n in the denominator has to be replaced by the value $(n - 1)$, and in the limit $(V_i - \langle V \rangle)^2 \ll \sigma_i^2$ the revised formula reduces to the regular expression for the standard errors of the average $\langle V \rangle$ obtained from n independent single measurements of V_i. For the data in Tables 7 and 8 the consistency is good, and the use of (8) is therefore justified.

Second pressure derivatives of effective second-order elastic constants. For calculating the second pressure derivatives, the isothermal first pressure derivative of the isothermal single-crystal bulk modulus is required. This derivative is found by using the general relation [*Thurston*, 1967]

$$(\partial K_0^S/\partial P)_T = (K_0^S)^2(S_{ppii}{}^S \beta_{ijkl}' S_{klmm}{}^S) \quad (9)$$

to determine the isothermal derivative of the adiabatic bulk modulus $(K_0^S)' = 9.63$ and then converting this value to the purely isothermal derivative $(K_0^T)' = 9.42$ by using *Barsch*'s [1967] equation 5. The quantities β_{ijkl}' appearing in (9) are the thermodynamic pressure derivatives of the single-crystal adiabatic elastic constants. The equations necessary to convert the measured effective derivatives to thermodynamic quantities have been given by *Thurston* [1965]. By using the equations of *Barsch and Frisillo* [1973], the second pressure derivatives of the effective elastic constants have been computed (Table 8). It should be noted that the quantities c_{44}'', c_{55}'', and c_{66}'' are negative but that the second derivatives c_{12}'', c_{13}'', and c_{23}'' of the cross-coupling moduli are positive. These positive values result from a change in sign when the negative values of $(\rho_0 W^2)''$ are subtracted in determining $(\rho V^2)''$, used in com-

TABLE 8. Isothermal Second Pressure Derivatives of the Adiabatic Effective Elastic Constants at 25°C

$c_{\mu\nu}$	Specimen	$\vec{N}$	$\vec{U}$	$[\partial^2(\rho_0 W^2)/\partial P^2]_0$, Mb^{-1}	$[\partial^2 c_{\mu\nu}{}^S/\partial P^2]_0$, Mb^{-1}	Weighted Average, Mb^{-1}
c_{44}	1	[010]	[001]	-30.0 ± 1.8	-31.5	
	4	[010]	[001]	-33.6 ± 2.3	-35.1	-28.1 ± 2.5
	1	[001]	[010]	-24.3 ± 1.6	-23.4	
	1*	[001]	[010]	-26.3 ± 2.4	-25.2	
c_{55}	1	[100]	[001]	-61.5 ± 1.6	-62.3	
	3	[100]	[001]	-54.1 ± 2.2	-55.0	-59.5 ± 2.2
	1	[001]	[100]	-59.1 ± 3.0	-57.8	
c_{66}	1	[100]	[010]	-17.0 ± 1.4	-18.1	
	3*	[100]	[010]	-13.4 ± 2.4	-14.7	-17.3 ± 1.2
	1	[010]	[100]	-17.2 ± 3.8	-18.6	
	4	[010]	[100]	-15.9 ± 1.9	-17.2	
c_{12}	2	[l m 0]	[$m\bar{l}$0]	-23.4 ± 2.2	49.3	(50.7)†
	2*	[l m 0]	[$m\bar{l}$0]	-25.1 ± 1.6	51.4	
c_{13}	4*	[l 0 n]	[n 0 $\bar{l}$]	-42.4 ± 4.7	64.4	(66.3)†
	4*	[l 0 n]	[n 0 $\bar{l}$]	-44.2 ± 5.5	68.8	
c_{23}	3	[0 m n]	[0 n $\bar{m}$]	-30.8 ± 3.0	64.4	(62.0)†
	3*	[0 m n]	[0 n $\bar{m}$]	-30.0 ± 5.1	68.8	

*Test made with Arenberg PSP AFC ultrasonic equipment. All other data taken with MRL PSP AFC equipment.

†Calculated by assuming c_{11}'', c_{22}'', and c_{33}'' to be zero.

puting the second pressure derivatives of the cross-coupling moduli, and from the assumption that the second pressure derivatives of the on-diagonal longitudinal moduli, which also enter the calculation, are zero. Although the change in sign follows from the equations used to compute the quantities $(\rho V^2)''$, it is important to note that any nonlinear behavior for the on-diagonal longitudinal moduli is not precluded by the present study, since the longitudinal data were very difficult to obtain at higher pressures where curvature might be observed. Because there is no reason to suspect that these coefficients behave linearly under pressure when the shear coefficients do not, it is likely that the second pressure derivatives of the on-diagonal longitudinal moduli are also nonzero. Consequently, the values and the signs of the second pressure derivatives of the cross-coupling moduli depend on the magnitude and the sign of the on-diagonal longitudinal modes. It is probable, therefore, that, although the determined values of $(\rho_0 W^2)''$ are excellent, the computed values for c_{12}'', c_{13}'', and c_{23}'' (Table 8) are considerably in error. As a result, a complete description of the nonlinear behavior of the bronzite specimens cannot be given in this study. One important conclusion resulting from the present data, however, is that the elastic properties of possible earth materials can show curvature even at pressures as low as 10 kb. However, owing to a solid-solid phase transition, which should occur at about 135 kb [*Ringwood*, 1967; *Ahrens and Gaffney*, 1971], the curvature in the bronzite data should not play a significant role in the earth's interior.

The stated errors for each run in Table 8 are the standard deviations resulting from fitting the data to a quadratic function in pressure. The weighted averages and their associated

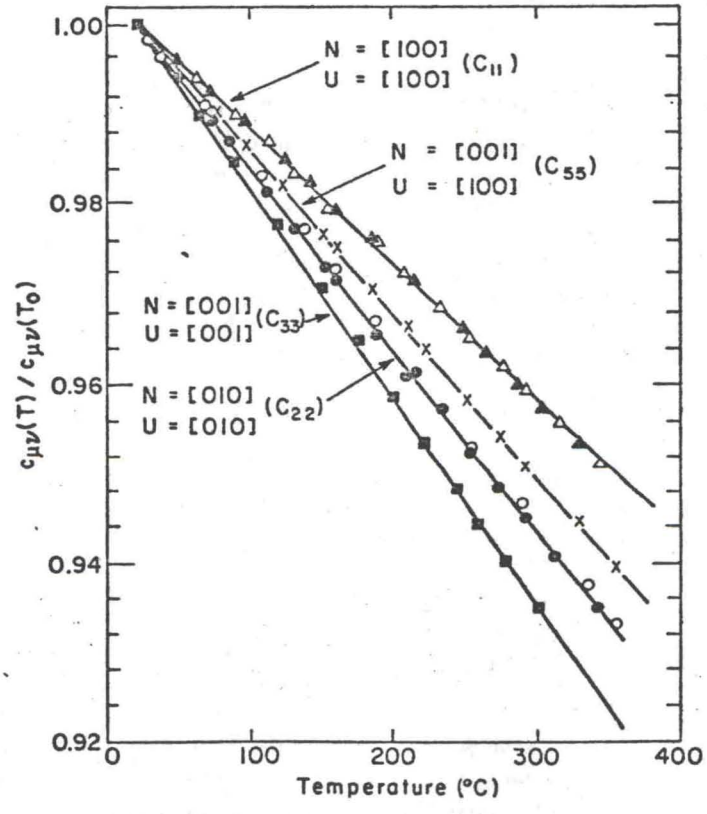

Fig. 4. Experimental data of the on-diagonal elastic constants c_{11}, c_{22}, c_{33}, and c_{55} (referred to their values at $T_0 = 25°C$) as a function of temperature. Solid triangles, solid squares, open circles, and crosses indicate specimen 1; open triangles, specimen 3; solid circles, specimen 4.

TABLE 9. Isobaric Temperature Derivatives of the On-Diagonal Elastic Constants at 25° to 350°C

Elastic Constant	Specimen	$\vec{N}$	$\vec{U}$	$(\partial c_{\mu\nu}{}^{S}/\partial T)_{p=0}$, kb °C^{-1}	Weighted Average, kb °C^{-1}
c_{11}	1	[100]	[100]	-0.352 ± 0.001	-0.352 ± 0.001
	3	[100]	[100]	-0.353 ± 0.001	
c_{22}	1	[010]	[010]	-0.328 ± 0.001	-0.328 ± 0.001
	4	[010]	[010]	-0.329 ± 0.001	
c_{33}	1	[001]	[001]	-0.516 ± 0.004	-0.516 ± 0.004
c_{44}	1	[001]	[010]	-0.128 ± 0.002	-0.131 ± 0.003
	4	[010]	[001]	-0.122 ± 0.002	
c_{55}	1	[001]	[100]	-0.138 ± 0.002	-0.138 ± 0.002
c_{66}	3	[100]	[010]	-0.133 ± 0.001	-0.145 ± 0.005
	4	[010]	[100]	-0.150 ± 0.005	

errors were determined by (7) and (8). The difficulty of accurately specifying the second pressure derivatives is reflected in the relatively large scatter in the present data. However, because this difficulty exists, even for synthetic single-crystal specimens (see, for example, *Chang and Barsch* [1971] and *Barsch and Shull* [1971]), and because four different naturally occurring specimens were used, the consistency of the determined second pressure derivatives must be considered as excellent.

As was mentioned above, cross checks on the second pressure derivatives of the cross-coupling moduli by using the quasi-longitudinal modes were not possible. Therefore the consistency of the results was examined by repeating the pressure runs for the quasi-shear modes. The reproducibility and the agreement of these data and those for c_{44}'' and c_{66}'' obtained by using two different sets of ultrasonic electronic equipment support the nonlinear elastic behavior of the shear moduli beyond any doubt.

Temperature dependence of second-order elastic constants at 1 atm. The temperature dependence of the quantities ρV^2, which are necessary to determine the temperature derivatives of the elastic constants, has been directly determined by making the appropriate density and length corrections. Because the on-diagonal elastic moduli are given by $c_{\mu\mu}{}^{S} = \rho V^2$, the temperature derivatives for $c_{\mu\mu}{}^{S}$ are explicitly determined by fitting a polynomial to the data for ρV^2 as a function of temperature. The temperature dependence of ρV^2 for the on-diagonal moduli c_{11}, c_{22}, c_{33}, and c_{55} is plotted in Figure 4. The values have been normalized by dividing by $c_{\mu\nu}(T_0)$, with $T_0 = 25°C$.

The values for the temperature derivatives of the on-diagonal elastic constants and their standard deviations as determined by a polynomial fit to these data are presented in Table 9. In all cases the temperature dependence was found to be linear, within experimental limits, up to 350°C. The equations necessary to calculate the temperature derivatives of the cross-coupling coefficients have been given by *Graham* [1969] and *Frisillo* [1972].

The experimental data necessary to compute the temperature dependence of the cross-coupling coefficients have been given by *Graham* ences of the values of ρV^2 for the quasi modes. These data, again normalized by dividing by the initial value $\rho_0 V_0^2$, are presented in Figure 5. The computed values for the derivatives of the

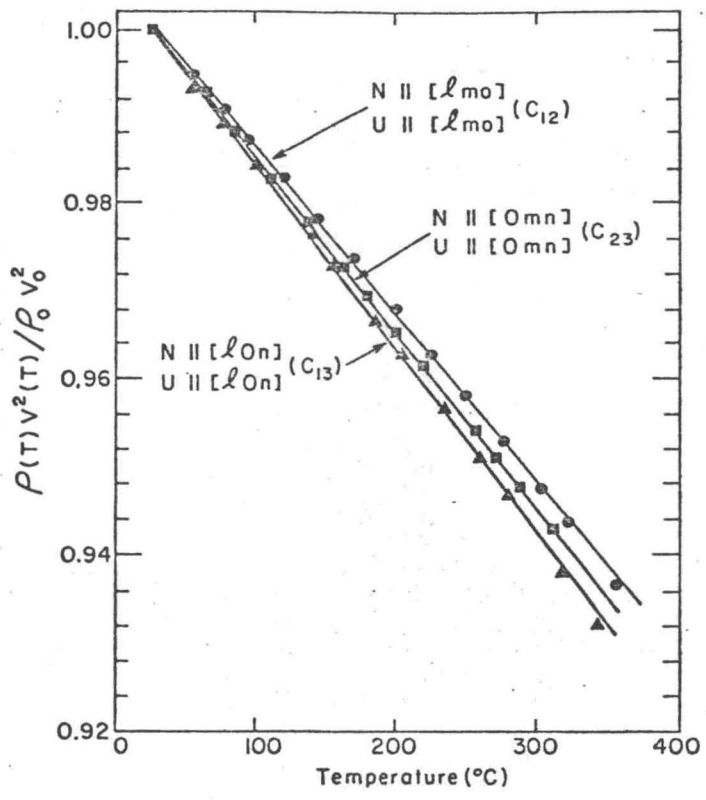

Fig. 5. Experimental data of ρV^2 (referred to the value at $T_0 = 25°C$) for the quasi-shear modes used to determine the cross-coupling moduli c_{12}, c_{13}, and c_{23} as a function of temperature. Circles indicate specimen 2; squares, specimen 3; triangles, specimen 4.

cross-coupling moduli are presented in Table 10. The stated errors and the weighted averages and their errors have been determined by using the error propagation method and (7) and (8), respectively.

Discussion

Comparison of bronzite data with those of other authors and for other materials of geophysical interest. The single-crystal elastic constants of orthopyroxene at room temperature and 1 atm have been measured previously by *Ryzhova et al.* [1966] and *Kumazawa* [1969]. The elastic constants of orthopyroxene from these authors are compared with the results presented here (Table 11). Because the specimen used by *Ryzhova et al.* [1966] had a large porosity (1.8%), their reported values are significantly low in some cases. The present data and those of Kumazawa, however, compare favorably, the elastic constants in the present study being somewhat smaller, apparently owing to the increased iron concentration. Because values for c_{33} and c_{12}, however, are higher than

TABLE 10. Isobaric Temperature Derivatives of the Cross-Coupling Elastic Constants at 25° to 350°C

Elastic Constant	Specimen	$\vec{N}$	$\vec{U}$	$[\partial(\rho V^2)/\partial T]_{p=0}$, kb °C^{-1}	$[\partial c_{\mu\nu}/\partial T]_{p=0}$, kb °C^{-1}
c_{12}	2	[ℓm0]	[ℓm0]	-0.417	-0.212 ± 0.007
c_{13}	4	[ℓ0n]	[ℓ0n]	-0.462	-0.318 ± 0.008
c_{23}	3	[0mn]	[0mn]	-0.388	-0.107 ± 0.007

TABLE 11. Comparison of Adiabatic Single-Crystal Elastic Constants $c_{\mu\nu}^S$ of Orthopyroxene with Those of Other Investigators at 25°C (All values in Mb.)

μν	Present Work ($Mg_{0.8}Fe_{0.2}SiO_3$)	*Kumazawa* [1969] ($Mg_{0.84}Fe_{0.16}SiO_3$)	*Ryzhova et al.* [1966] (Not Analyzed)
11	2.286	2.299	1.876
22	1.605	1.654	1.578
33	2.104	2.057	2.085
44	0.8175	0.8306	0.700
55	0.7548	0.7637	0.592
66	0.776	0.7853	0.544
12	0.710	0.701	0.586
13	0.548	0.573	0.605
23	0.460	0.496	0.561

those of Kumazawa, careful consideration was given to checking the n conditions for these modes that might cause such disagreement. No such error was found in the present study.

The isotropic elastic constants of bronzite and their derivatives with respect to pressure and temperature as calculated from the single-crystal data by means of the Voigt-Reuss-Hill (VRH) approximation are compared with some experimental data on polycrystalline bronzite containing 10% enstatite [*Chung*, 1971] (Table 12). Also included for comparison in this table are the isotropic properties of 20% fayalite olivine obtained by *Graham* [1970] by linearly extrapolating his single-crystal data on the pure end-member Mg_2SiO_4 [*Graham and Barsch*, 1969] and those of *Kumazawa and Anderson* [1969] on $(Mg_{0.93}Fe_{0.07})_2SiO_4$. In addition, isotropic elastic-property data of garnet of the almandine pyrope variety [*Soga*, 1967] are presented. It is apparent that the densities, the bulk moduli, and the shear moduli of the two bronzite specimens are rather similar but that the values of $(\partial K^S/\partial P)_T$ differ by almost a factor of 2. Without further systematic work on well-characterized polycrystalline specimens, any attempt to explain this large discrepancy would be merely speculative. The elastic data

TABLE 12. Comparison of Isotropic Moduli and Pressure and Temperature Derivatives of Bronzite ($Mg_{0.8}Fe_{0.2}SiO_3$) with Those of Polycrystalline Bronzite ($Mg_{0.9}Fe_{0.1}SiO_3$), Olivine, and Garnet at 25°C

Parameter	Bronzite*	Bronzite, 10% Enstatite†	Olivine, 20% Fayalite§	Almandine-Pyrope Garnet¶
ρ_0, g/cm³	3.354	3.273	3.459	4.160
K^S, Mb	1.035	1.06	1.256	1.770
K^T, Mb	0.9878		1.226	1.757
$(\partial K^S/\partial P)_T$	9.59	5.3	5.09	5.43
$(\partial K^T/\partial P)_P$	9.47		5.16	5.45
$(\partial K^S/\partial T)_P$, kb/°C	-0.268		-0.193	-0.201
$(\partial K^T/\partial T)_P$, kb/°C	-0.296		-0.223	-0.201
G, Mb	0.755	0.768	0.788	0.943
$(\partial G/\partial P)_T$	2.38		1.74	1.400
$(\partial G/\partial T)_P$, kb °C	-0.119		-0.142	-0.106

*From this study.
†From *Chung* [1971].
§From *Graham* [1970].
¶From *Soga* [1967].

of olivine differ somewhat but not greatly from the present bronzite data, except in the value of $(\partial K^s/\partial P)_T$, for which a difference of a factor of about 2 occurs. Because the Fe/Mg ratio in both materials is approximately the same, this difference is attributed to the different crystal structures. Although the composition of the garnet specimen differs considerably from the compositions of the bronzite and olivine samples (it corresponds to an almandine to pyrope ratio of about 3:1), the pressure coefficients of the bulk modulus and of the shear modulus are closer to the values for the olivine sample. The contrast with the bronzite data underlines again the unusual properties of the enstatite structure.

It is important to note that, from the compression data of *Bridgman* [1948] on hypersthene, an equally large value for the isothermal first pressure derivative of the bulk modulus is obtained. Bridgman's data are expressed in the form $(V_0 - V)/V = aP + bP^2$, where V_0 and V are the specimen volumes at ambient and elevated pressures, respectively, $a = 1.08$ Mb^{-1}, $b = 5.2$ Mb^{-2}, and $\rho_0 = 3.42$ g/cm^3 for the hypersthene sample studied. The isothermal bulk modulus and its isothermal pressure derivative are obtained from the relations [*Anderson*, 1966] $K^T = 1/a = 0.9259$ Mb and $(\partial K^T/\partial P)_T = 2b(K^T) - 1 = 7.9$. Although Bridgman's data are less accurate than the present acoustic data, the large value of $(\partial K^T/\partial P)_T$ obtained from his measurements is indicative of the anomalous behavior of orthopyroxene at high pressure.

Incomplete velocity measurements as a function of temperature and pressure have also been performed on natural rock specimens containing primarily bronzite [*Hughes and Nishitake*, 1963; *Birch*, 1960; *Simmons*, 1964]. These data have been combined by *Anderson and Sammis* [1970] to give the complete set of data of the velocities and their derivatives with respect to temperature and pressure (Table 13). The results calculated from the present single-crystal data by means of the VRH average are also shown for comparison. Although, because of porosity, heterogeneity, and grain size, the accuracy of data from natural rock specimens is usually not very good, the two sets of data shown in Table 13 are in fair agreement.

Nonlinearity of pressure dependence. In Figure 6 the pressure dependence of the on-diagonal shear moduli is plotted as calculated from the measured elastic data according to the linear approximation

$$c_{\mu\nu} = c_{\mu\nu}^0 + (\partial c_{\mu\nu}/\partial P)_0 P \qquad (10)$$

and according to the quadratic approximation

$$c_{\mu\nu} = c_{\mu\nu}^0 + (\partial c_{\mu\nu}/\partial P)_0 P + (\partial^2 c_{\mu\nu}/\partial P^2)_0 (P^2/2) \qquad (11)$$

It is apparent that, at pressures above about 20–30 kb, considerable deviations from the linear relation (10) arise as a result of the quadratic term in (11) and that, for c_{44} and c_{55}, maximums occur at about 85 and 50 kb, respectively. Without knowledge of the derivatives higher than second order or of the convergence of the Taylor expansion of the elastic constants with respect to pressure or both, it is, of course, not possible to establish the exact functional dependence on pressure in the range considered. Because calculations for alkali halides based on model potentials show that the exact pressure dependence falls between the linear dependence and the quadratic dependence [*Barsch and Shull*, 1971], it is not unreasonable to expect qualitatively similar behavior for bronzite. Thus for two of the three on-diagonal shear moduli a substantial deviation from nonlinearity would remain, even if the quadratic terms would be reduced, for example, to half their values.

The remaining shear moduli are functions of the on-diagonal longitudinal moduli c_{11}, c_{22}, and c_{33}, of the cross-coupling moduli c_{12}, c_{13}, and c_{23}, and of the direction cosines of the propagation direction. Because it was not possible to measure the second pressure derivatives of the on-diagonal

TABLE 13. Comparison of Present Bulk Velocity Data Obtained by Using VRH Averages with Those Measured in Bronzite Rock Samples

Parameter	Present Data	*Anderson and Sammis* [1970]*
ρ, g/cm^3	3.354	3.279
V_P, km/sec	7.78	7.64
V_S, km/sec	4.72	5.59
$(\partial V_P/\partial P)_T$, 10^{-3} km/sec kb	20.57	19.00
$(\partial V_P/\partial T)_P$, 10^{-4} km/sec °C	-9.08	-6.40
$(\partial V_S/\partial P)_T$, 10^{-3} km/sec kb	5.16	7.00
$(\partial V_S/\partial T)_P$, 10^{-4} km/sec °C	-4.86	-6.00

*Based on data from *Hughes and Nishitake* [1963], *Birch* [1960], and *Simmons* [1964].

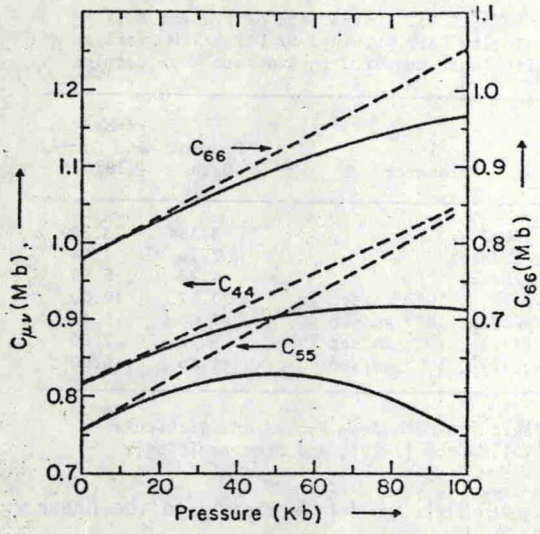

Fig. 6. Pressure dependence of on-diagonal shear constants. Dashed lines indicate linear extrapolation; solid lines, quadratic extrapolation.

longitudinal moduli, the second pressure derivatives of these shear moduli are still unknown. However, because the nonlinearity found for the quasi-shear modes (see, for example, the curve for **N** || [*l*0*n*] and **U** || [*n*0$\bar{l}$] in Figure 3) and the second pressure derivatives of the cross-coupling moduli determined from the assumption $(\partial^2 c_{\mu\mu}/\partial P^2) = 0$ ($\mu = 1, 2, 3$, no summation) (Table 6) are of the same order of magnitude as those of the on-diagonal shear moduli, it is to be expected that the second pressure derivatives of the remaining shear moduli are of the same order of magnitude. By the same token, the second pressure derivatives of the isotropic shear modulus, which depend in the VRH approximation on the second pressure derivatives of all nine elastic constants, should be expected to be roughly equal to the average of the second pressure derivatives of the on-diagonal shear moduli (approximately -33 Mb^{-1}). In connection with the values of the isotropic shear modulus (0.75 Mb) and its first pressure derivative (2.38), it is thus apparent that, at the highest pressures of the stability range of orthopyroxene (about 90–135 kb [*Ringwood*, 1967; *Akimoto and Syono*, 1970; *Ahrens and Gaffney*, 1971]), small deviations for a nonlinear pressure dependence may become noticeable and should be included in accurate geophysical applications.

To compare the magnitude of the second pressure derivatives of the elastic constants with the corresponding values of other materials, it is convenient to consider the dimensionless quantity $K^T(\partial^2 c_{\mu\nu}/\partial P^2)$. With $K^T = 0.988$ Mb and the data of Table 8, this quantity is seen to range from -14 to -57 for the three on-diagonal shear moduli. For the eight alkali halides for which the second pressure derivatives of the elastic constants have been measured and which represent both the rocksalt and the cesium chloride structures, the quantity $K^T(\partial^2 c_{44}/\partial P^2)$ ranges from -1 to -4.5 [*Chang and Barsch*, 1967, 1971; *Barsch and Shull*, 1971]. For spinel a value of -5.5 has been measured [*Chang and Barsch*, 1972]. Thus the values reported here for bronzite appear to be anomalously large. An explanation of this behavior requires a lattice theoretical analysis based on the crystal structure of enstatite, similar to the analysis presented for spinel by *Striefler and Barsch* [1972]. Although such an analysis is not yet available, it appears plausible to attribute the large curvature to the phase transition or the disproportionation of enstatite between about 90 and 135 kb [*Akimoto and Syono*, 1970; *Ahrens and Gaffney*, 1971]. The decrease of the shear moduli at pressures above the maximums displayed in Figure 6 indicates decreasing mechanical stability paralleled by decreasing thermodynamic stability and the occurrence of a phase transformation before the mechanical stability limit (e.g., if the quadratic extrapolation is used, $c_{55} = 0$ at $P \cong 220$ kb) is reached.

Compression of bronzite at very high pressures. The ultrasonic equation of state has been calculated from the present bronzite data by using the first-order Birch equation (Figure 7). For illustrative purposes only, the nonlinear elastic data for bronzite have also been extrapolated by using the second-order Birch equation of state. These data are also included in Figure 7. Although the nonlinear data are quite uncertain, it is interesting to note that the deviation from the linearly extrapolated data is quite small at 150 kb. If geophysical applications where temperature effects are important to depths of >200 km are considered, it is unlikely that this small difference caused by the curvature will play an important role in the equation of state. This conclusion is no longer valid, of course, if the orthopyroxene-garnet transition does not occur and the stability

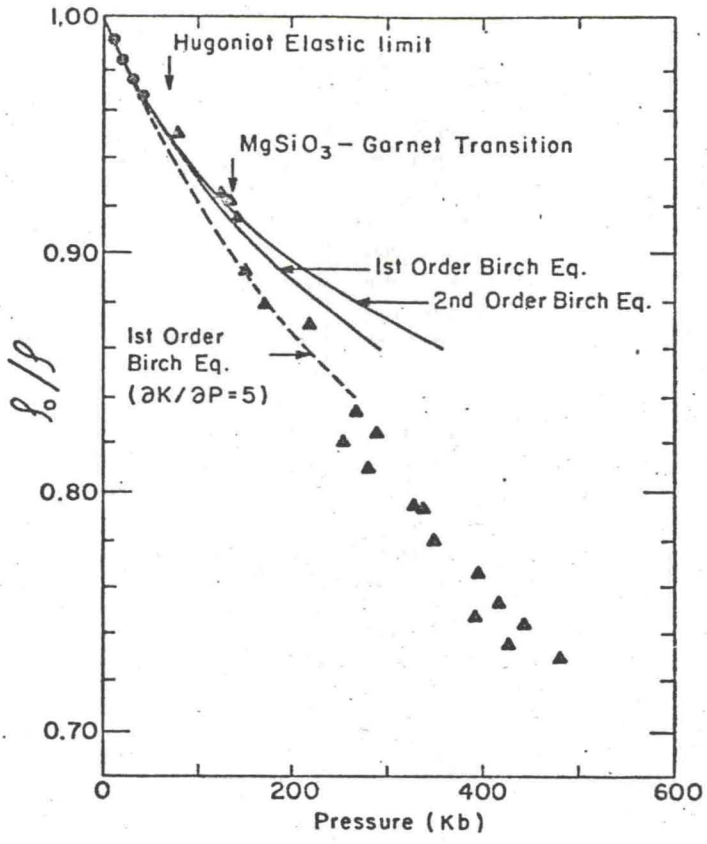

Fig. 7. Comparison of ultrasonic equation of state for bronzite calculated from Birch's equations with static-compression data of *Bridgman* [1948] (circles) and shock-wave data of *Ahrens and Gaffney* [1971] (triangles and dashed lines).

range of the orthopyroxene structure extends to higher pressures, say, to about 200–300 kb, or if the nonlinearity of the on-diagonal longitudinal constants turns out to be very large.

In addition to the acoustic measurements of this study, isothermal-compression data on hypersthene to 40 kb [*Bridgman*, 1948] and shock-compression data on Bamle enstatite [*Ahrens and Gaffney*, 1971] have been included in Figure 7 for comparisoin. Although a direct comparison with the present data is not possible because the shock data are not isothermal, it is worthy to note that the three shock points between the Hugoniot elastic limit, where enstatite should behave plastically, and approximately 150 kb are in reasonable agreement with the present data. Further examination of the shock data in the 150-kb regions shows a discontinuity indicative of a possible phase transition. By constructing an enstatite isentrope with *Kumazawa's* [1969] value of the adiabatic bulk modulus and an assumed low pressure derivative of 5.0, *Ahrens and Gaffney* [1971] argued that the final Hugoniot states above a level of approximately 135 kb lie at a greater density than that indicated for the enstatite isentrope. By converting their values used for calculating the enstatite isentrope to isothermal quantities, the extrapolated curve also shown in Figure 7 was obtained. However, when the present data are compared with the shock-compression values, the discontinuity is more convincingly illustrated, and thus the interpretation of a phase transition in the vicinity of 135 kb is supported.

Pressure dependence of lattice parameters. *Thurston* [1967] has proposed an equation of state that permits the calculation of the lattice parameters a_i ($i = 1, 2, 3$) as a function of pressure from the principal stretches λ_i according to

$$\lambda_i = \frac{a_i(P)}{a_i^0} = \left[1 + \left(\frac{\partial K^T}{\partial P}\right)_T \frac{P}{K^T}\right]^{m_i} e^{n_i P} \quad (12)$$

$$i = 1, 2, 3$$

The index 0 refers to zero pressure. The parameters m_i and n_i depend on the isothermal elastic compliances and the isothermal pressure derivatives of the isothermal effective elastic constants according to (I, 88), (I, 90), (II, 9), and (II, 15) of *Thurston* [1967]. Their numerical values as calculated from the experimental data of Tables 6 and 7 are listed in Table 14. Also included in this table are the zero pressure lattice parameters a_i^0 as determined from X-ray measurements in this laboratory [*Frisillo and Buljan*, 1972] (these values agree quite closely with those reported by *Wyckoff* [1968] for $Mg_{0.465}Fe_{0.535}SiO_3$, namely, $a_0 = 18.310$ A, $b_0 = 8.927$ A, and $c_0 = 5.226$ A) and the linear compressibilities $\alpha_i = (\partial \ln a_i/\partial P)_T$ and their pressure coefficients $\beta_i = (\partial \alpha_i/\partial P)_T$ as calculated from the data of Tables 6 and 7 on the basis of (I, 88) and (I, 90) of *Thurston* [1967]. In Figure 8 the principal stretches and the lattice parameters as calculated from (12) are plotted as a function of pressure. No directly measured data are available for comparison.

Although Thurston's equation of state (12) is a generalization of Murnaghan's equation of state and is therefore based on the linear approximation for the elastic constant versus pressure relation, its range of validity may be more limited because it is based on equation (II, 10) of *Thurston* [1967] as an additional assumption. Although Thurston's equation has been verified for several materials up to pressures of about 30% of the bulk modulus [*Thurston*, 1967] and for Al_2O_3 up to pressures of 10% of the bulk modulus [*Gieske and Barsch*, 1968], discrepancies have been reported for Mg_2SiO_4 (forsterite) [*Olinger and Duba*, 1971]. Apart from such experimental errors in the high-pressure X-ray data of *Olinger and Duba* [1971] as may result from nonhydrostatic stresses in their opposed anvil system, the possibility cannot be ruled out that the discrepancies arise from the fact that equation (II, 10) of *Thurston* [1967] does not hold for forsterite. For this reason the pressure dependence of the lattice parameters (Figure 8) should be considered as a plausible prediction only, until Thurston's equation (12) is tested for a larger variety of materials. Additional errors may arise from neglecting the quadratic terms in the pressure dependence of the elastic constants and from using the isothermal pressure derivatives of the adiabatic elastic constants (Table 7) instead of the unknown isothermal pressure derivatives of the isothermal elastic constants. Both errors, however, may be expected to be small.

With these reservations about the dependability of Thurston's equation (12) in mind, one can conclude from Figure 8 that the compression behavior of the three orthorhombic axes is noticeably different. Especially noteworthy is the rapid decrease of the slope of the curve for the c axis, which indicates a rapid decrease of the linear compressibility in this direction. At 200 kb, for example, the linear compressibility of the c axis is 3 and 6 times smaller than the linear compressibilities of the a and b axes, respectively. Undoubtedly, this behavior arises from the special features of the crystal structure of enstatite. This structure consists of SiO_4 chains extending along the c direction and interconnected by the (Mg, Fe) cations [*Wyckoff*, 1968]. Thus, although the initial linear compressibilities along the different crystallographic

TABLE 14. Zero Pressure Lattice Parameters a_i^0, Linear Compressibilities α_i, Pressure Coefficients β_i, and Exponents m_i and n_i of Thurston's Equation of State

Axis	i	a_i^0, A	α_i, Mb^{-1}	β_i, Mb^{-2}	m_i	n_i, Mb^{-1}
a	1	18.262	-0.2344	1.858	-0.02000	-0.04448
b	2	8.870	-0.4375	3:603	-0.03783	-0.07828
c	3	5.203	-0.3303	4.411	-0.04771	0.12276

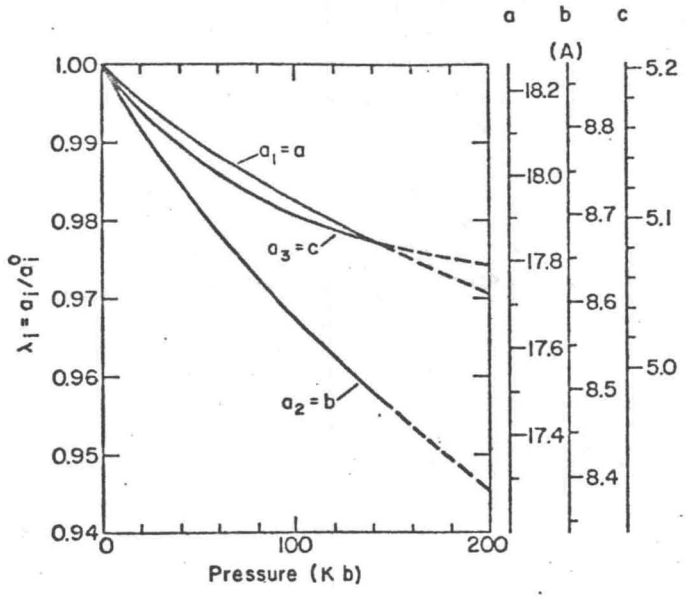

Fig. 8. Principal stretches λ_i and lattice parameters a_i of bronzite versus pressure from ultrasonic elastic data according to Thurston's equation of state. Here $a_0 = 18.262$ A, $b_0 = 8.870$ A, and $c_0 = 5.203$ A.

axes differ by only 30%, at higher compressions the linear compressibility of the c axis appears to be reduced by the greater stiffness of the SiO_4 chains against further compression.

Debye temperature and Grueneisen parameter. The isotropic elastic constant data (Table 12) can be used to calculate the elastic Debye temperature θ according to [*Anderson*, 1965]

$$\theta = h/k[(3p/4\pi)(N\rho/M)]^{1/3}v_m \qquad (13)$$

where h and k are Planck's constant and Boltzmann's constant, respectively, p is the number of ions per primitive unit cell (5 for enstatite), N is Avogadro's number, and M is the molecular weight. The mean sound velocity v_m is given by [*Anderson*, 1965]

$$v_m = [(v_p^{-3} + 2v_S^{-3})/3]^{-1/3} \qquad (14)$$

and v_p and v_s are the longitudinal and shear velocities, respectively (Table 13). The low- and high-temperature limits γ_0 and γ_∞ of the elastic Grueneisen parameter can be calculated approximately from [*Anderson et al.*, 1968]

$$\gamma_0 = (\Delta^3\gamma_P + 2\gamma_S)/(\Delta^3 + 2) \qquad (15a)$$

$$\gamma_\infty = (\gamma_P + 2\gamma_S)/3 \qquad (15b)$$

where $\Delta = v_S/v_P$ and γ_P and γ_S are the average Grueneisen parameters of the longitudinal and shear modes, respectively [*Anderson et al.*, 1968]:

$$\gamma_P = \tfrac{1}{3} + (K_T/v_P)(\partial v_P/\partial P)_T \qquad (16a)$$

$$\gamma_S = \tfrac{1}{3} + (K_T/v_S)(\partial v_S/\partial P)_T \qquad (16b)$$

where $(\partial v_P/\partial p)_T$ and $(\partial v_S/\partial p)_T$ are the pressure gradients of the velocities listed in Table 13.

The quantities calculated according to (13), (15), and (16) are $\theta = 724$°K, $\gamma_P = 3.09$, $\gamma_S = 1.48$, $\gamma_0 = 1.65$, and $\gamma_\infty = 2.02$. Because no experimental specific heat data of bronzite are available, the elastic Debye temperature cannot be compared with its thermal value.

The room temperature value of the thermal Grueneisen parameter

$$\gamma = \beta K_T/\rho c_V \qquad (17)$$

is 1.56, calculated from the experimental value of the volume thermal expansion coefficient $\beta = 4.70\ 10^{-5}$ °K^{-1} [*Frisillo and Buljan*, 1972] and from a value of $c_V = 94.50$ joule mole^{-1} °K^{-1}, which was calculated from the elastic Debye temperature on the basis of the Debye function [*Beattie*, 1926]. As has been observed for numerous other (but not all) solids, the elastic and

thermal Grueneisen parameters γ_x and γ agree surprisingly well. This agreement shows that bronzite belongs to that large class of materials for which the average over all vibrational modes of the crystal required for the calculation of the Grueneisen parameter in the quasi-harmonic approximation [*Barron*, 1955] can be successfully approximated by the directional average of the elastic modes, the dispersion and the contributions from the optical branches thereby being neglected.

Because γ_0 is only 18% smaller than γ_x, it appears that the temperature variation of the Grueneisen parameter is small. A small temperature dependence of γ has been observed for many (but not all) oxide compounds [*Anderson et al.*, 1968].

SUMMARY AND CONCLUSIONS

The dependence of the nine single-crystal elastic constants of bronzite on pressure and temperature was measured and showed several unusual features. The first pressure derivative and the temperature derivative of the longitudinal modulus in the crystallographic c axis and the first pressure derivative of the bulk modulus are anomalously large. These results are consistent with earlier polycrystal data and compression measurements of Bridgman. The linear compressibility of the c axis decreases much more rapidly with increasing pressure than the linear compressibilities of the other two axes. All these phenomena seem to arise from the more rapid stiffening upon compression of the SiO_4 chains parallel to the c axis and constituting the crystal structure of enstatite. In addition, the pressure dependence of the shear velocities along the three crystallographic axes, of the velocities of the quasi-shear modes along directions forming angles of approximately 45° with these directions, and of the associated shear moduli were found to be noticeably nonlinear below 10 kb. This phenomenon is attributed to the decreasing stability of the enstatite structure with increasing pressure, which results in a phase transformation or in disproportionation into spinel and stishovite. On the other hand, other properties, such as the magnitude and the temperature dependence of the thermal Grueneisen parameter and its agreement with the elastic Grueneisen parameter, are entirely normal.

APPENDIX: LEAST-SQUARES FIT OF $\rho_0 W^2$ TO A POLYNOMIAL OF DEGREE N IN PRESSURE

The pressure derivatives of the effective elastic constants were determined from the expansion coefficients A_n^N of the quantity $\rho_0 W^2$ as defined by

$$\rho_0 W^2 = \rho_0 \sum_{n=0}^{N} A_n^N (P^n/n!) \qquad \text{(A1)}$$

The degree N of the polynomial to which a given set of data points for a particular mode was fitted was determined on the basis of three criteria.

First, the total sum of the least-squares deviation $[vv]$ for a fit of $\rho_0 W^2$ to a polynomial of degree N must be significantly smaller (say, at least 3 times) than that of a polynomial of degree $N - 1$ and not significantly larger (say, at most 3 times) than that of a polynomial of degree $N + 1$.

Second, the coefficients $t_n^N = A_n^N/\Delta A_n^N$, where ΔA_n^N denotes the standard error of the nth-order expansion coefficient for a fit to a polynomial of degree N, must obey the standard Student t test [*Draper and Smith*, 1966] for a probability of 0.95. Because all runs consist of 16–18 data points of $\rho_0 W^2$ (with the exception of one run consisting of only 11 data points), the degrees of freedom for $N = 1, 2$, and 3 range from 13 to 17, and the coefficient t_n^N for a probability of 0.95, according to the tables for the standard t test [*Draper and Smith*, 1966], must be larger than about 2.1–2.2.

Third, the coefficients A_n^N and especially the highest-order coefficients A_N^N obtained from independent measurements and representing different modes belonging to the same elastic modulus must be consistent within their joint standard error.

The application of these criteria is illustrated for the shear and quasi-shear modes. As can be seen from Table A1, the total sum of the least-squares deviation $[vv]$ is, for the fit to a quadratic relation ($N = 2$), 2.6–46 times smaller than that for the fit to a linear relation ($N = 1$), whereas, for the fit to a third-order polynomial ($N = 3$) $[vv]$ is reduced by only a small amount ranging from 1 to 70%. Thus the first criterion, with the exception of one mode, is satisfied for a fit to a quadratic relation.

In Table A2 the quantities t_n^N (for the coefficient of P^2 for the fit to a quadratic relation

TABLE A1. Sum of Least-Squares Deviation $[vv]$ for Least-Squares Fit of W^2 to a Polynomial in Pressure of Degree N for Shear and Quasi-Shear Modes

Coefficient	$\vec{N}$	$\vec{U}$	Sample	$N = 1$, 10^{-9} cm^2/sec^2	$N = 2$, 10^{-9} cm^2/sec^2	$N = 3$, 10^{-9} cm^2/sec^2
c_{44}	[010]	[001]	1	25.5	1.15	0.94
	[010]	[001]	4	33.4	1.96	1.92
	[001]	[010]	1*	20.1	1.02	0.32
	[001]	[010]	1	18.7	1.00	0.49
c_{55}	[100]	[001]	1	12.1	1.22	1.02
	[100]	[001]	3	88.2	1.92	0.88
	[001]	[100]	1	116.6	4.43	2.31
c_{66}	[100]	[010]	1	9.23	0.93	0.66
	[100]	[010]	3*	6.93	1.98	1.05
	[010]	[100]	1	13.1	5.02	4.19
	[010]	[100]	4	8.52	1.31	1.07
c_{12}	$[lmo]$	$[m\bar{l}o]$	2*	18.0	0.89	0.83
	$[lmo]$	$[m\bar{l}o]$	2	17.7	0.73	0.62
c_{13}	$[lon]$	$[no\bar{l}]$	4*	43.1	5.62	4.43
	$[lon]$	$[no\bar{l}]$	4*	48.5	7.67	7.61
c_{23}	$[omn]$	$[on\bar{m}]$	3*	29.7	3.26	3.01
	$[omn]$	$[on\bar{m}]$	3	27.2	7.00	5.91

*Run made with Arenberg PSP AFC equipment. All other data were taken with MRL PSP AFC equipment.

and for the coefficients of P^2 and P^3 for the fit to a third-order polynomial) required for the Student t test are listed for all shear and quasi-shear modes. It is apparent that, for the fit to the quadratic relation, all quantities t_n^N meet the Student t test for 95% probability ($t_2^2 > 2.1$). For the fit to a third-order polynomial, the Student t test for 95% probability is not fulfilled for either one or both of the quantities t_2^3 and t_3^3 for most modes, with the exception of modes 4, 6, and 7, for which $t_2^3 > 2.1$ and $t_3^3 > 2.1$. According to Table A1, for these three modes the reduction of $[vv]$ in changing from a fit to a quadratic relation in pressure to a cubic one is relatively large and amounts to about 50%. Because the limit of about 70% reduction assumed in the first criterion is subjective and could as well be taken as 50%, these three modes represent borderline cases, and, by relaxing the standards of the first criterion slightly, their fit to a third-order polynomial could be justified statistically. On the other hand, the corresponding t values of the coefficients of P^2 (i.e., $n = 2$) are for $N = 2$ over twice as large as those for $N = 3$, and the coefficients are therefore more precise for $N = 2$ than for $N = 3$. Thus one has the choice of fitting these modes to a second-order polynomial with standard errors of the coefficients of P^2 ranging from 4 to 7% or of fitting them to a third-order polynomial with standard errors of the coefficients of P^2 and P^3 amounting to about 12 and 27%, respectively. A decision between these two possibilities cannot be made on the basis of the first two criteria. As will be shown below, the third criterion is also fulfilled for fitting these modes to a third-order polynomial. Because all other shear and quasi-shear modes were fitted to second-order polynomials, it was decided to fit modes 4, 6, and 7 for the sake of uniformity to second-order polynomials also. It should be pointed out, however, that this assumption is an ad hoc one and introduces a truncation error of unknown magnitude. As will be shown below, this truncation error may, for the coefficients of P^2 for the pure shear modes, be as large as 50% but is likely to be smaller than this value.

For the discussion of the third criterion, the expansion coefficients A_n^N as defined by (A1) and their standard errors for $N = 2$ and $n = 2$, $N = 3$ and $n = 2$, and $N = 3$ and $n = 3$ for all shear and quasi-shear modes are listed in Table A3. Also listed are the average values $\langle A_n^N \rangle$ of all modes belonging to the same elastic modulus and their standard errors Δ calculated

TABLE A2. Quantities $t_n^N = A_n^N/\Delta A_n^N$ for Student's t Test for Coefficients of Least-Squares Fit of $\rho_0 W^2$ to a Polynomial in Pressure of Degree N according to $\rho_0 W^2 = \sum_{n=0}^{N} A_n^N P^n$ for $N = 2$ and $N = 3$

Coefficient	Mode No.	$\vec{N}$	$\vec{U}$	Sample	$N = 2$ and $n = 2$	$N = 3$ and $n = 2$	$N = 3$ and $n = 3$
c_{44}	1	[010]	[001]	1	16.59	4.62	1.63
	2	[010]	[001]	4	14.45	2.96	0.51
	3	[001]	[010]	1*	10.96	4.86	1.30
	4	[001]	[010]	1	15.10	7.12	3.55
c_{55}	5	[100]	[001]	1	38.37	8.51	1.61
	6	[100]	[001]	3	24.15	9.73	3.78
	7	[001]	[100]	1	19.67	8.26	3.72
c_{66}	8	[100]	[010]	1	11.60	0.25	2.40
	9	[100]	[010]	3*	5.70	1.93	3.27
	10	[010]	[100]	1	4.59	2.34	1.53
	11	[010]	[100]	4	8.45	0.07	1.66
c_{12}	12	$[l m 0]$	$[m\bar{l}0]$	2*	10.26	2.76	1.00
	13	$[l m 0]$	$[m\bar{l}0]$	2	5.88	2.47	1.43
c_{13}	14	$[l 0 n]$	$[n0\bar{l}]$	4*	8.95	0.002	1.72
	15	$[l 0 n]$	$[n0\bar{l}]$	4*	7.99	1.64	0.30
c_{23}	16	$[0 m n]$	$[0n\bar{m}]$	3*	15.84	3.60	0.90
	17	$[0 m n]$	$[0n\bar{m}]$	3	10.64	1.96	0.64

*Run made with Arenberg PSP AFC ultrasonic equipment. All other data were taken with MRL PSP AFC equipment.

from $\Delta = \{[vv]/p(p-1)\}^{1/2}$, where $[vv]$ is the sum of the squares of the p individual modes from the average value $\langle A_n^N \rangle$. These quantities characterize the consistency of the various modes for the same modulus.

The third criterion can be quantitatively stated as the condition that, for internal consistency, the standard errors Δ must be smaller than or of approximately the same magnitude as the standard errors of the individual modes obtained from the least-squares data fit.

From the data in Table A3 it is evident that for $N = 2$ the consistency for all shear and quasi-shear modes is good to very good. For $N = 3$ the coefficients of P^2 and P^3 are still consistent for the modes belonging to the moduli c_{44}, c_{55}, c_{12}, and c_{13}, but for the moduli c_{66} and c_{23} the coefficients are not consistent. In spite of the consistency found for $N = 3$ for the moduli c_{44}, c_{55}, c_{12}, and c_{13}, only a fit corresponding to $N = 2$ will be used in these cases, since the data have been shown not to meet at least one of the first and second criteria.

It is also apparent from the data in Table A3 that in changing from $N = 2$ to $N = 3$ the magnitude of the coefficient of P^2 (i.e., A_2^N) is increased by about 50%. The values of A_2^N for $N = 4$ (not included in Table A3) lie between

TABLE A3. Expansion Coefficients A_n^N with Standard Errors of W^2 according to (A1) for Shear and Quasi-Shear Modes

Coefficient	Mode No.	$\vec{N}$	$\vec{U}$	Sample	$N = 2$ and $n = 2$, 10^{-8}cm^2 sec^{-2} kb^{-2}	$N = 3$ and $n = 2$, 10^{-8}cm^2 sec^{-2} kb^{-2}	$N = 3$ and $n = 3$, 10^{-8}cm^2 sec^{-2} kb^{-3}
c_{44}	1	[010]	[001]	1	-447 ± 27	-685 ± 148	16 ± 10
	2	[010]	[001]	4	-501 ± 35	-605 ± 205	7 ± 13
	3	[001]	[010]	1*	-392 ± 36	-486 ± 100	10 ± 8
	4	[001]	[010]	1	-361 ± 24	-711 ± 100	22 ± 6
	Average				-425 ± 31	-622 ± 51	14 ± 3
c_{55}	5	[100]	[001]	1	-917 ± 24	-1127 ± 132	13 ± 8
	6	[100]	[001]	3	-806 ± 33	-1306 ± 134	32 ± 8
	7	[001]	[100]	1	-881 ± 45	-1584 ± 192	46 ± 12
	Average				-868 ± 33	-1339 ± 96	31 ± 10
c_{66}	8	[100]	[010]	1	-253 ± 22	30 ± 119	-19 ± 8
	9	[100]	[010]	3*	-200 ± 35	298 ± 155	-32 ± 10
	10	[010]	[100]	1	-257 ± 56	-723 ± 309	30 ± 20
	11	[010]	[100]	4	-237 ± 28	10 ± 151	-16 ± 10
	Average				-237 ± 13	-385 ± 459	-9 ± 50
c_{12}	12	$[l m 0]$	$[m \bar{l} 0]$	2*	-459 ± 45	-714 ± 256	17 ± 17
	13	$[l m 0]$	$[m \bar{l} 0]$	2	-448 ± 76	-1037 ± 419	40 ± 21
	Average				-454 ± 35	-876 ± 115	29 ± 8
c_{13}	14	$[l 0 n]$	$[n 0 \bar{l}]$	4*	-632 ± 71	1 ± 374	-44 ± 25
	15	$[l 0 n]$	$[n 0 \bar{l}]$	4*	-659 ± 83	-806 ± 491	10 ± 33
	Average				-646 ± 10	-403 ± 285	-17 ± 19
c_{23}	16	$[0 m n]$	$[0 n \bar{m}]$	3*	-375 ± 24	-498 ± 139	8 ± 9
	17	$[0 m n]$	$[0 n \bar{m}]$	3	-349 ± 33	395 ± 201	2 ± 3
	Average				-362 ± 9	-52 ± 315	5 ± 2

*Run made with Arenberg PSP AFC ultrasonic equipment. All other data were taken with MRL PSP AFC equipment.

those for $N = 2$ and $N = 3$, and it is therefore reasonable to expect that an increase of 50% represents an upper bound for the truncation error. To eliminate or reduce the truncation error for A_2^N, all measurements would have to be extended to substantially higher pressures and the data fitted to a polynomial of degree N greater than 3 or 4, such that this fit would still be statistically significant and A_2^N would become independent of N within its standard deviation. This task remains for the future.

Acknowledgments. We would like to thank Drs. Z. P. Chang and H. E. Shull and Mr. P. L. Carcia for technical advice and Mrs. J. Schiff for the computer work in connection with the data analysis. Our thanks are extended to Dr. E. K. Graham for bringing to our attention P. W. Bridgman's compression data on hypersthene. Further, Mr. H. H. Demarest's suggestion of equation 8 for the error calculation and a fruitful discussion with Dr. B. L. Joiner and Miss K. McKim of the Pennsylvania State University Statistical Consulting Service on nonlinear regression analysis and on the applicability of (8) are gratefully acknowledged.

This work was supported by the National Science Foundation under grant GA 3985.

REFERENCES

Ahrens, T. J., and E. S. Gaffney, Dynamic compression of enstatite, *J. Geophys. Res., 76,* 5504–5513, 1971.

Akimoto, S. I., and Y. Syono, High-pressure decomposition of the system $FeSiO_3$-$MgSiO_3$, *Phys. Earth Planet. Interiors, 3,* 186–188, 1970.

Alexandrov, K. A., and T. V. Ryzhova, The elastic properties of rock-forming minerals, 1, Pyroxenes and amphiboles, *Bull. Acad. Sci. USSR. Geophys. Ser.,* no. 9, 871–875, 1961.

Alexandrov, K. A., T. V. Ryzhova, and B. P. Belikow, The elastic properties of pyroxenes, *Soviet Phys. Crystallogr.,* no. 8, 589–591, 1963.

Anderson, D. L., and C. Sammis, Partial melting in the upper mantle, *Phys. Earth Planet. Interiors, 3,* 41–50, 1970.

Anderson, O. L., Determination and some uses of isotropic elastic constants of polycrystalline aggregates using single crystal data, in *Physical Acoustics,* vol. 3B, edited by W. P. Mason, pp. 43–95, Academic, New York, 1965.

Anderson, O. L., The use of ultrasonic measurements under modest pressure to estimate compression at high pressures, *J. Phys. Chem. Solids, 27,* 547–565, 1966.

Anderson, O. L., E. Schreiber, R. L. Liebermann, and N. Soga, Some elastic constant data on minerals relevant to geophysics, *Rev. Geophys. Space Phys., 6,* 491–524, 1968.

Barron, T. H. K., On the thermal expansion of solids at low temperatures, *Phil. Mag., 46,* 720–734, 1955.

Barsch, G. R., Adiabatic, isothermal and intermediate pressure derivatives of the elastic constants for cubic symmetry, 1, Basic formulae, *Phys. Status Solidi, 19,* 129–138, 1967.

Barsch, G. R., and A. L. Frisillo, Determination of second pressure derivatives of elastic constants from elastic wave velocities for orthorhombic, tetragonal, trigonal, hexagonal, and cubic symmetry, *J. Acoust. Soc. Amer., 46,* in press, 1973.

Barsch, G. R., and H. E. Shull, Pressure dependence of elastic constants and crystal stability of alkali halides, NaI and KI, *Phys. Status Solidi, 43,* 637–649, 1971.

Beattie, J. A., Six place tables of the Debye energy and specific heat functions, *J. Math. Phys. Cambridge Mass., 6,* 1–32, 1926.

Bechmann, R., The elastic piezoelectric and dielectric constants of piezoelectric crystals, in *Landolt-Börnstein, Numerical Data and Functional Relationships in Science and Technology,* vol. 2, *Group III: Crystal and Solid State Physics,* edited by K. H. Hellwege, pp. 40–101, Springer, New York, 1969.

Birch, F., The velocity of compressional waves in rocks to 10 kilobars, 1, *J. Geophys. Res., 65,* 1038–1102, 1960.

Bogardus, E. H., Elastic anharmonicity in germanium, magnesium oxide and fused silica, Ph.D. thesis, 117 pp., Pa. State Univ., University Park, 1964.

Bridgman, P. W., Rough compression on 177 substances to 40,000 kg/cm², *Proc. Amer. Acad. Arts Sci., 76,* 71–87, 1948.

Chang, Z. P., and G. R. Barsch, Nonlinear pressure dependence of elastic constants and fourth-order elastic constants of cesium halides, *Phys. Rev. Lett., 19,* 1381–1383, 1967.

Chang, Z. P., and G. R. Barsch, Pressure dependence of the elastic constants of RbCl, RbBr and RbI, *J. Phys. Chem. Solids, 32,* 27–40, 1971.

Chang, Z. P., and G. R. Barsch, Pressure dependence of single-crystal elastic constants and anharmonic properties of spinel, submitted to *J. Geophys. Res.,* 1972.

Chung, D. H., Equations of state of pyroxenes in the (Mg, Fe)SiO_3 system (abstract), *Eos Trans. AGU, 52,* 919, 1971.

Draper, N., and H. Smith, *Applied Regression Analysis,* p. 305, John Wiley, New York, 1966.

Fisher, E. S., and H. J. McSkimin, Adiabatic elastic moduli of single-crystal alpha uranium, *J. Appl. Phys., 29,* 1473–1484, 1958.

Frisillo, A. L., The elastic coefficients of bronzite as a function of pressure and temperature, Ph.D. thesis, 170 pp., Pa. State Univ., University Park, 1972.

Frisillo, A. L., and S. T. Buljan, The linear thermal expansion coefficients of orthopyroxene to 1000°C, *J. Geophys. Res., 77,* in press, 1972.

Gieske, J. H., The third order elastic coefficients and some anharmonic properties of aluminum oxide, Ph.D. thesis, 133 pp., Pa. State Univ., University Park, 1968.

Gieske, J. H., and G. R. Barsch, Pressure dependence of the elastic constants of single crystalline aluminum oxide, *Phys. Status Solidi, 29,* 121–131, 1968.

Graham, E. K., The elastic coefficients of forsterite as a function of pressure and temperature, Ph.D. thesis, 161 pp., Pa. State Univ., University Park, 1969.

Graham, E. K., Elasticity and composition of the upper mantle, *Geophys. J. Roy. Astron. Soc., 20,* 285–302, 1970.

Graham, E. K., and G. R. Barsch, Elastic constants of single-crystal forsterite as a function of temperature and pressure, *J. Geophys. Res., 74,* 5949–5960, 1969.

Hearmon, R. F. S., The elastic constants of nonpiezoelectric crystals, in *Landolt-Börnstein, Numerical Data and Functional Relationships in Science and Technology,* vol. 2, *Group III: Crystal and Solid State Physics,* edited by K. H. Hellwege, pp. 1–39, Springer, New York, 1969.

Hughes, D. S., and T. Nishitake, Measurement of elastic wave velocities in Armco iron and jadite under high pressures and high temperatures, *Geophysical Papers Dedicated to Professor Kenzo Sassa,* pp. 379–385, Geophysical Institute, Kyoto University, Kyoto, Japan, 1963.

Kumazawa, M., The elastic constants of single-crystal orthopyroxene, *J. Geophys. Res., 74,* 5973–5980, 1969.

Kumazawa, M., and O. L. Anderson, The elastic moduli, pressure derivatives, and temperature derivatives of single-crystal olivine and single-crystal forsterite, *J. Geophys. Res., 74,* 5961–5972, 1969.

McSkimin, H. J., Pulse superposition method for measuring ultrasonic wave velocities in solids, *J. Acoust. Soc. Amer., 33,* 12–16, 1961.

Miller, D. L., Precision measurement of the elastic constants of solids and their temperature and pressure variation, Ph.D. thesis, 80 pp., Pa. State Univ., University Park, 1969.

Olinger, B., and A. Duba, Compression of olivine to 100 kilobars, *J. Geophys. Res., 76,* 2610–2616, 1971.

Overton, W. C., Jr., Relation between ultrasonically measured properties and the coefficients in the solid equation of state, *J. Chem. Phys., 37,* 116–119, 1962.

Ringwood, A. E., The pyroxene-garnet transformation in the earth's mantle, *Earth Planet. Sci. Lett., 2,* 255–263, 1967.

Ryzhova, T. V., K. S. Alexandrov, and V. M. Korobkova, The elastic properties of rock-forming minerals, 5, Additional data on silicates, *Izv. Acad. Sci. USSR Phys. Solid Earth,* no. 2, 111–113, 1966.

Simmons, G., Velocity of shear waves in various minerals to 10 kilobars, *J. Geophys. Res., 69,* 1117–1130, 1964.

Soga, N., Elastic constants of garnet under pressure and temperature, *J. Geophys. Res., 72,* 4227–4234, 1967.

Striefler, M., and G. R. Barsch, Lattice dynamics of zero wave vector and elastic constants of spinel in the rigid ion approximation, *J. Phys. Chem. Solids, 33,* in press, 1972.

Thurston, R. N., Effective elastic coefficients for wave propagation in crystals under stress, *J. Acoust. Soc. Amer., 37,* 348–356, 1965.

Thurston, R. N., Calculation of lattice-parameter changes with hydrostatic pressure from third-order elastic constants, *J. Acoust. Soc. Amer., 41,* 1093–1111, 1967.

Thurston, R. N., and K. Brugger, Third order elastic constants and the velocity of small amplitude elastic waves in homogeneously stressed media, *Phys. Rev., 133,* A1604–A1610, 1964.

Wyckoff, R. G. W., *Crystal structures,* vol. 4, *Miscellaneous Inorganic Compounds, Silicates and Basic Structural Information,* chapter XII.B, p. 301, Interscience, New York, 1968.

(Received February 7, 1972;
revised August 2, 1972.)